MEASUREMENT OF UNBALANCED RESPONSE IN A SFD TEST ROTOR KIT, PART II

Hector Loas

Dr. San Andres

May 1995

TRC-RD-5-95

Texas A&M University
Mechanical Engineering Department

Measurements of Unbalance Response in a SFD Test Rotor Kit, Part II

by

Hector Laos
graduate research assistant

A Research Progress Report
to the
Turbomachinery Research Consortium

May 1995

TRC Project:
Experimental and Analytical Study of the Non-Linear Response of Squeeze Film Damper Supported Rotors.
Principal Investigator: Dr. Luis San Andres, Associate Professor

TABLE OF CONTENTS

Abstract

Measurements of the unbalance response in a squeeze film damper (SFD) rotor-kit are presented. A complete description of the test rig, instrumentation, and data acquisition process are provided. Results from the measurements of the system unbalance response are presented for three cases: centered journal, offcentered journal at 30% of the radial clearance and offcentered journal at 60% of the radial clearance. For each case different unbalance masses are used. All the experiments were performed with a light oil temperature of 29.5° C and an oil inlet pressure of 3.5 10^4 Pa. The cascade plots show no trace of any asynchronous vibrations, except for the journal offcentered at 60% of the radial clearance. For this last case a supersynchronous vibration tracked the unbalance response at about twice the rotational speed. A commercial rotordynamics code (PUP) was used to obtain the damping coefficients at the damper support. The damping coefficients were obtained by trial and error using the criteria to match the model with the experimental results. This process was successful as shown in the comparisons between the experimental data and the rotordynamic model. The rotor deflected shapes of the centered journal- unbalance response were calculated using the rotordynamic model to predict the amplitude of vibrations at the SFD location. Using the values previously calculated as data, the damping coefficients were evaluated using equations for the centered and non-cavitated damper. Finally the damping coefficients for the offcentered cases were predicted for an uncavitated SFD. The ratio of extracted to theoretical damping coefficients from the rotor kit ranges from 1.3 to 2.9. That is, the test rotor-kit provides more damping than theoretical predictions.

Introduction

Jet engines exhibit a trend toward high rotational speeds, generating unbalance forces that produce high vibration levels on the rotating system when this is supported only on rolling element bearings. Squeeze film dampers (SFD's) aid in reducing the amplitude of vibration due to rotor unbalance by introducing a viscous damping mechanism, and also increase the life of the antifriction rolling element bearings. In industry, SFD's are used along with tilting-pad bearings when more damping is needed to suppress rotordynamic instabilities.

A SFD consists of a non-rotating journal rigidly attached to a rolling element bearing and within a rigid housing. The annular gap between journal and its housing is filled with a lubricant. Often the journal and its centering spring are constructed as a single unit as shown in the Figure 1. The journal whirls due to the effect of the unbalance or other dynamic force excitations in a rotor. Due to the action of the centering spring the journal describes an orbit, with amplitudes of motion bounded by the film clearance.

The forces produced by the SFD affect in many ways the behavior of a rotor - bearing system. For high levels of unbalance theory predicts an increase on the whirl amplitude, effect that can be potentially dangerous in an aircraft engine. The increase of the oil film pressure will prevent cavitation in the oil film, but the high levels of oil inlet pressure necessary to achieve good results makes this concept very difficult to apply in turbomachinery. The oil film pressure in the SFD "rotates" inside the damper and in this way air enter the damper when the dynamic pressures are bellow ambient values . This effect is called "air entrainment", it is most difficult to predict, but can be prevented with the use of end seals. The magnitude of the SFD forces are directly related to the orbit of motion of the journal. It follows then that a SFD can never be located close to a modal node. Also, a SFD can be "locked up" if the oil used on the damper is of large viscosity . In general, it is necessary to make a careful analysis of the SFD characteristics in order to for it to work properly.

Squeeze film dampers are thought to be highly non-linear hydrodynamic devices (Ehrich, 1992). Linear and non-linear vibrating systems behave differently as shown in the following example for a simple rotor with linear supports. This system produces an unbalance response as shown in Figure 2 by the curve labeled linear viscous damper. Rotors supported on SFD's produce, theoretically, bistable-operation (and jump phenomena) created by the hardening stiffness effect of the SFD. This non-linear effects are shown by the curve labeled cavitated SFD on the same figure.

Thus, SFD's do not provide only damping but also could introduce undesirable non-linear characteristics that adversely affect the performance of a rotating system. However, experience has shown that the dynamic forced response of SFD's is very complex, and generally measurements have not correlated well with analytical predictions. For most

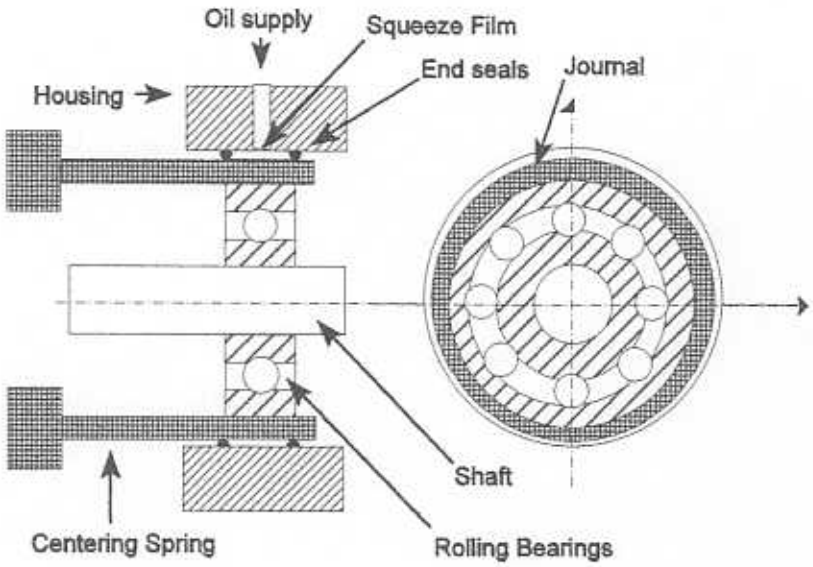

Figure 1. Squeeze film damper with centering spring

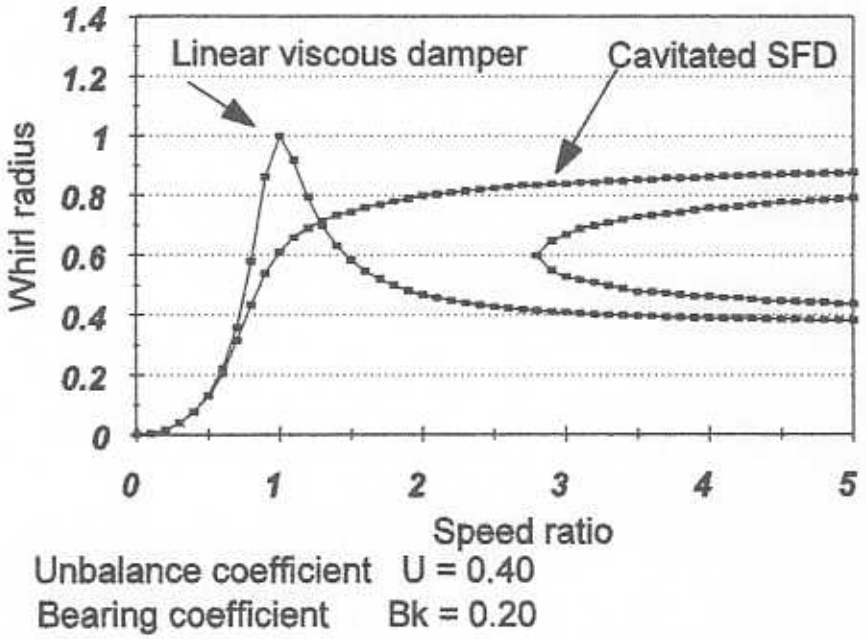

Figure 2. Unbalance response of a rigid rotor supported on a linear viscous damper and a cavitated SFD (π film model)

aircraft gas turbine applications, test results are strongly in conflict with Reynolds-equation predictions (Childs, 1993).

The profusion of theoretical results addressing to the non-linear aspects of rotors mounted on SFD's, has motivated the design and construction of a small test apparatus for the measurement of the dynamic forced response of a rotor supported on open-ends SFD's with centering springs. The experimental set-up has been kept simple enough to provide a means for correlation with analytical predictions but at the same time considering the important aspects of a practical application.

This research progress report presents a description of the SFD test apparatus and the measurements performed to identify the effects of SFD forces on the dynamic response of a rotating structural system. The test rig mechanical components are presented along with a description of the SFD element. The test procedure and instrumentation for collection of dynamic motion data for coastdown tests at a controlled deceleration rate are presented. Measurements of the dynamic forced response for the centered and offcentered journal cases with different disk unbalance levels are presented and discussed in detail. The unbalance response of the system is calculated using a commercial rotordynamics and the results are compared with the experimental data. The damping coefficients used for the theoretical modeling are presented for the centered and offcentered journal cases.

Description of rotor-SFD test apparatus

The following description of the test apparatus is taken from a previous technical report (San Andres, Laos and Lopez, (1994)). Figure 3(a) shows a photograph of the test apparatus and instrumentation used on the investigation, and Figure 3(b) describes the mechanical elements shown on figure 3(a). This last Figure clearly shows in the foreground the test rig apparatus (1) mounted on a base plate (13) inside the oil sump (14). The controller boxes (3) are located in another table. The equipment is supported by an aluminum plate (15) that is 25.4 mm (1 inch) thick and connected to a steel frame (16) mounted on vibration isolators (not shown). The instrumentation and the oil supply system will be described later.

Figure 4 depicts a cross-sectional view of the rotor and squeeze film damper along with the notation used to identify the system major components. The test apparatus consists of a steel shaft supported at two locations and with an overhung disk attached at one of the shaft ends. The configuration resembles that of a cantilever (overhung) rotor and effectively simulates a geometrical arrangement found in the aft compressor section in aircraft engines. The rotating system is connected with a flexible coupling to a variable speed DC motor with a top speed of 10,000 rpm and nominal power equal to 74.6 W (1/10 HP). At the driving motor end, the steel shaft of diameter (d) 9.52 mm.(3/8 in.) is supported with a brass bearing bushing backed with an elastomeric element (O'ring). The

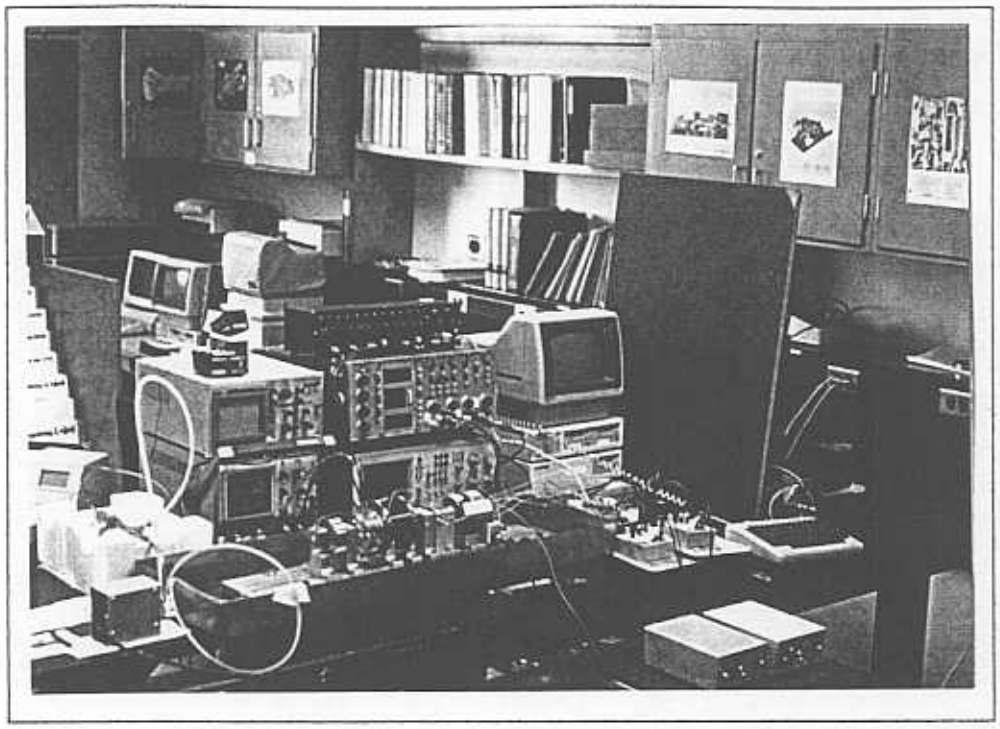

(a)

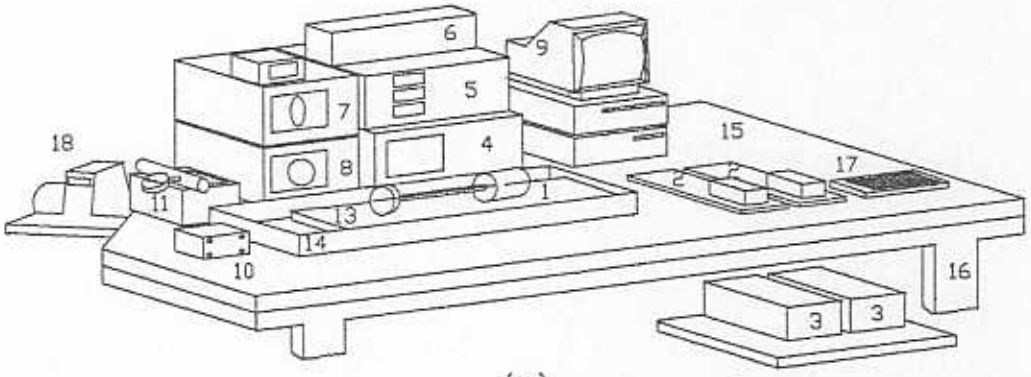

(b)

1 TEST RIG APPARATUS
2 PROXIMITORS
3 CONTROLLER BOX
4 SIGNAL ANALYZER
5 DIGITAL VECTOR FILTER
6 SIGNAL CONDITIONER
7 OSCILLOSCOPE (P1)
8 OSCILLOSCOPE (P3)
9 HP 9000 COMPUTER
10 OIL PUMP
11 PRESSURE GAUGE
12 THERMOCOUPLE
LCD DISPLAY
13 TEST RIG BASE
14 OIL RESERVOIR
15 ALUMINIUM PLATE
16 TABLE SUPPORT
17 KEYBOARD
18 HP PLOTTER

Figure 3 (a) Picture of the test rig apparatus and instrumentation (b) Description of the parts

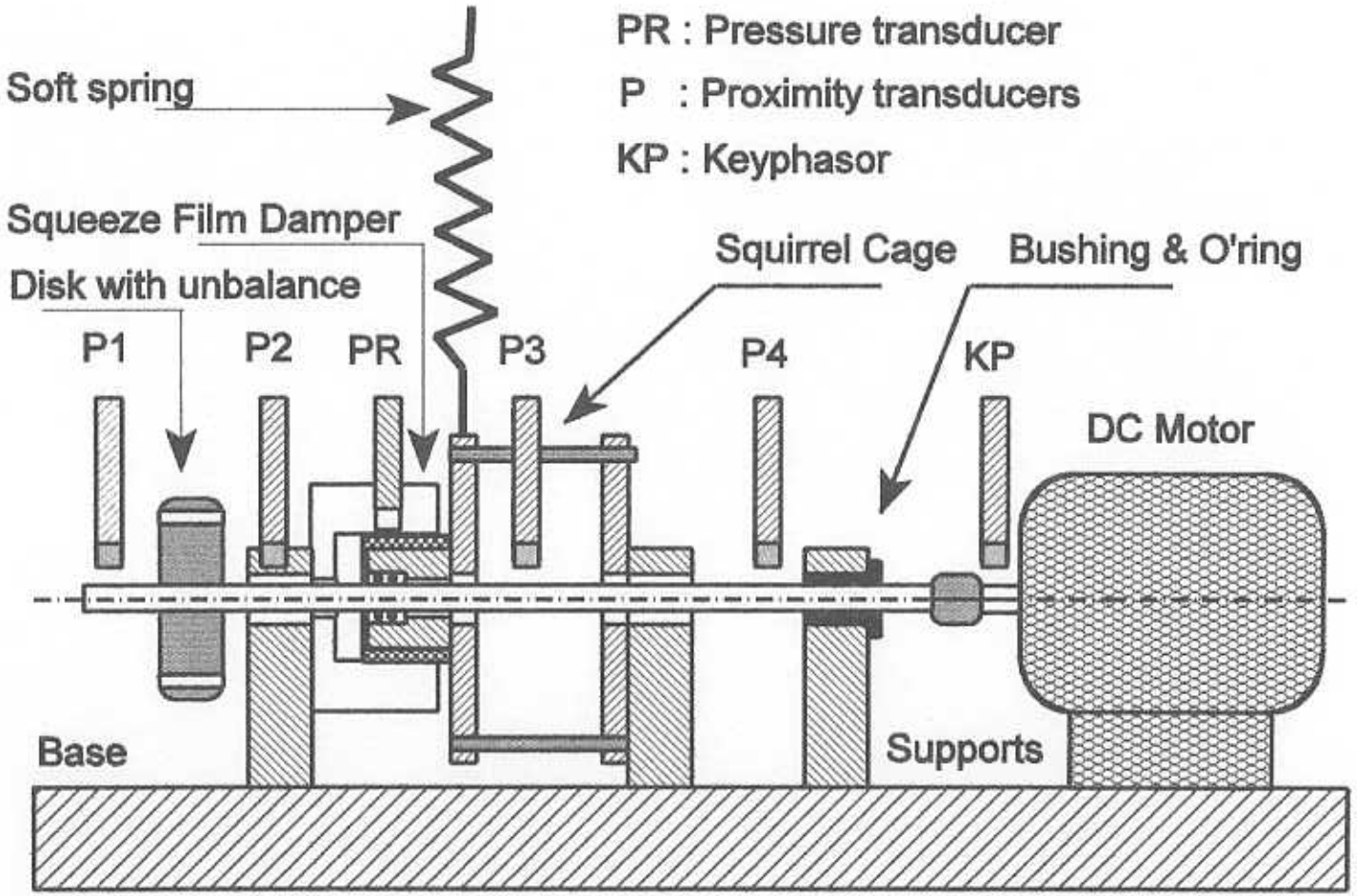

Figure 4. Rotor-Squeeze Film Damper Test Apparatus

stiffness of this support (K_S) was measured to be 148,858 ±3,275 N/m (850 lb/in) with an uncertainty of ±3,102 N/m (±18.70 lb/in)

The squeeze film damper (SFD) and shaft support squirrel cage structure are shown in Figure 5. Four soft steel rods are connected on one of their sides to a base structure, while the other sides are attached to a cylindrical steel body also working as the journal of the squeeze film damper. The shaft is pressed fitted on two ball bearings which are inserted with a tight fit on the interior surface of the journal. The journal also has an inserted outer race with a high quality surface finish. The weight of the journal and ball bearings (W_J) is equal to 7.96 N (1.79 lbs) with an uncertainty of ±0.22 N (0.05 lb). Static force versus deflection measurements of the squirrel cage determined values of structural stiffness (K_{SFD}) equal to 148,858 ±3,275 N/m (850 lb/in) and 143,604 ±3,102 N/m (820 lb/in) in the vertical and horizontal directions, respectively. To offcenter the journal relative to the damper a small force is applied to the base plate of the journal. This force is applied through a very soft spring (376 N/m (2.15 lb/in)) with an uncertainty of ± 7.15 N/m (±0.04lb/in)) and without affecting the stiffness of the squirrel cage. The journal can be moved inside the damper a maximum of 279.4 μm (11 mils) in the radial direction. The measure of the offcentering of the journal was made using a proximity probe with an uncertainty of ±1.27 μm (±0.05 mils).

The squeeze film damper element consists of a plexiglass housing connected rigidly to an aluminum support (see Figure 5). The inner surface of the housing fits loosely into the outer surface of the journal connected to the squirrel cage. The damper nominal length (l) and diameter (D) are equal to 25.4 mm (1.0 in.) and 50.8 mm (2.0 inch.) respectively. The uncertainty of this last measurements is ±0.01 mm (±0.005 inches). The radial film clearance (C) is equal to 0.28 mm (11 mils) with a variation of out-of -roundness of +/- 0.04 mm (1.5 mils). The squeeze film damper has both ends open to ambient conditions, and its geometric L/D and D/C ratios are equal to 0.5 and 200 respectively. Lubricant is fed to the damper housing midplane top section via a capillary tube providing a high flow resistance to avoid back-flow through the fluid supply lines. A small gear pump (maximum flow 1.21 lt/min (0.32 GPM) and 0.08 MPa (12 psi)) is used to deliver the lubricant to the damper, and a thermocouple and pressure gauge are installed just upstream of the capillary flow inlet. The lubricant used in the experiments corresponds to a Mobil No.3 oil with a specific gravity equal to 0.81 and viscosity values (μ) of 0.0028 Pa-s and 0.001784 Pa-s at 20°C and 40°C (68°F and 104°F) , respectively. Most experiments were carried out at an inlet oil temperature equal to 29.5°C (85°F) with a corresponding lubricant viscosity (μ_N) equal to 0.00225 Pa-s. The uncertainty on viscosity measurements is ± 0.00050 Pa-s.

The end disk, with a weight (W_D) of 7.96 N (1.79 lbs) (uncertainty of ±0.22 N (0.05 lb)), and a diameter (D_D) and width (l_D) equal to 76.2 and 25.4 mm. (3 and 1 inches) , respectively, has a series of machined holes spaced 22.5° apart at a radius (r) equal to

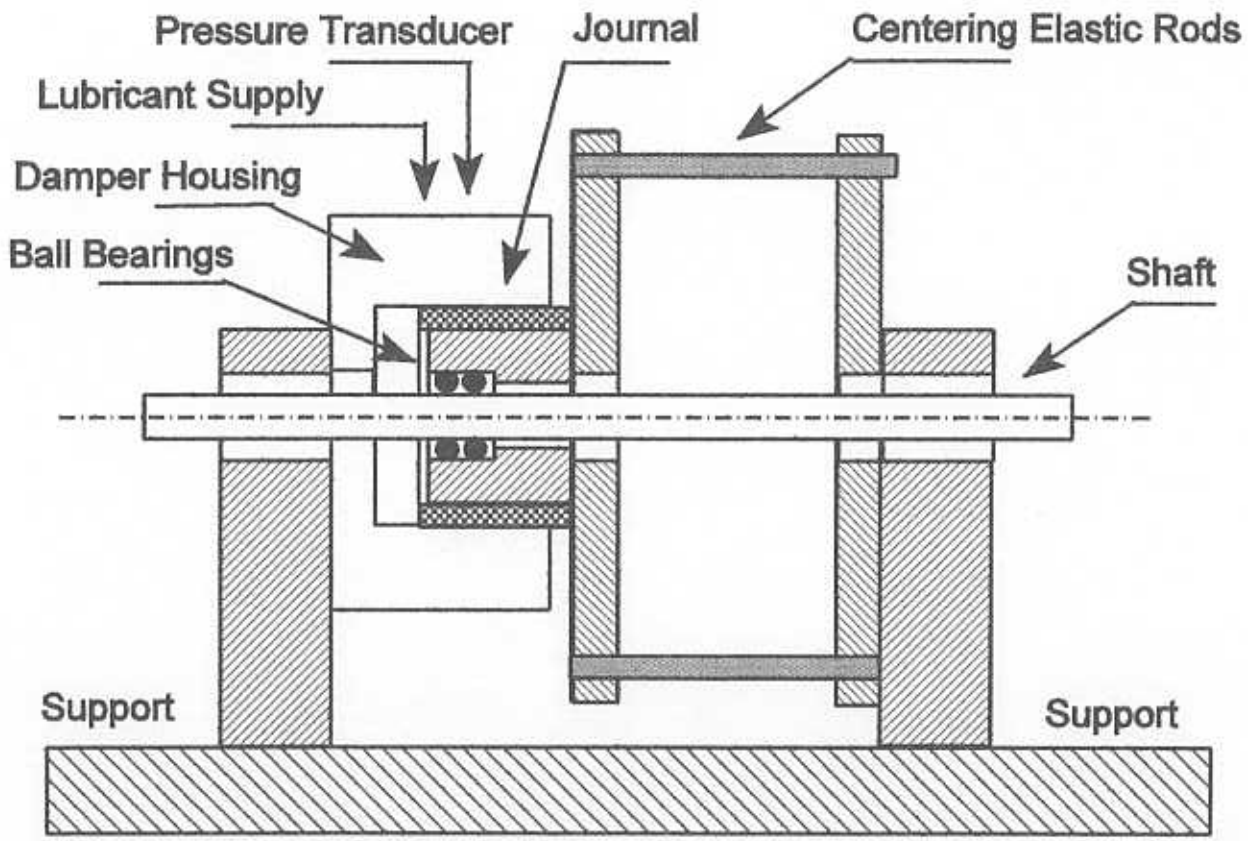

Figure 5. Squeeze Film Damper and Squirrel Cage Assembly

30.5 mm. (1.2 inches). The uncertainty of this measurements is ±0.01 mm (±0.005 inches). Calibrated weights can be inserted on these holes to provide a controlled unbalance force to excite dynamically the rotor-damper system. Pairs of non-contacting displacement sensors of the eddy current type are located at different positions on the test rig. The sensors are orthogonally positioned (vertical-Y and horizontal-X directions) at designated locations 1 through 4 as shown in Figures 4 and 6. Location 1 is closest to the end disk while location 4 is just next to the brass bushing and O'ring support. Locations 2 and 3 are on the sides of the squeeze film damper element. Two additional displacement sensors are positioned next to the driving motor, one provides a keyphasor signal and the other one is used for feedback control of the driving DC motor speed. Table 1 summarizes the characteristics of the elements previously described. Table 2 presents a list of the position of the transducers relative to the right end of the shaft (closest to the motor).

Description of the instrumentation

A data acquisition system (DAS) is used to collect vibration data while the rotor coastdown at a constant deceleration rate for different levels of unbalance masses at the end disk. A schematic view of the major pieces of instrumentation used on the investigation are shown on Figures 3(a) and 3(b), while Figure 7 shows the way they are connected with each other. A digital vector filter (4) takes the signal directly from the proximitors (2) and outputs the peak to peak amplitude of the vibration signal in direct or filtered modes. For the last case the output will also contain the phase angle associated with the reference mark on the shaft that is observed by the keyphasor. The typical gain of the proximity probes used is 200 mV / mil (8 mV / μm). The signal conditioner (6) is an electronic device that adjusts the signal from the proximitors in order to be used by other instruments.

Orbital shaft motions at locations 1 and 3 are displayed continuously on the oscilloscopes (7) and (8) and the spectrum analyzer (4) shows the frequency content of the shaft vertical and horizontal motions at locations P1 and P3. Also, the digital vector filter and the spectrum analyzer are connected directly to an HP-9000 series computer (9) via a HP-IB interface. The ADRE 2 rotordynamics software is used to collect and analyze the dynamic response of the rotor at only one shaft location per test (X-Y rotor displacements typically at locations P1 and P3), to calculate frequency spectrums, cascade plots, as well as to direct storage and access of the acquired data from the test apparatus for further manipulation. The color plotter (18) is used along with the ADRE system.

The lubricant inlet temperature and pressure (kept constant on the experiments) of the SFD are permanently monitored at the thermocouple LCD display (12) and the pressure gauge (11). The oil reservoir (14) contains about 3.78 lts (1 galon) of lubricant. Visual observations of the flow within the damper film lands are possible since the damper housing is transparent. A piezo-electric pressure transducer is inserted at the top of the transparent housing and is used to collect data of the oil film pressure. Table 3 shows the

Table 1. SFD-rotor kit components

Nomenclature	Description	Dimensions English unit	SI unit
C	Radial film clearance	11 mils	0.28 mm.
d	Diameter of the shaft	3/8 inch.	9.50 mm.
D	Damperl diameter	2.0 inch.	50.80 mm.
L	Damper length	1.0 inch	25.40 mm.
D_D	Disk diameter	3.0 inch.	76.20 mm.
K_S	O'ring bronze bushing stiffness	850 lb/inch	148,858 N/m
K_{SFD}	Squirrel cage stiffness	V: 850 lb/inch H 820 lb/inch	148,858 N/m 143,604 N/m
l	Damper nominal length	1.0 inch.	25.40 mm.
l_D	Disk nominal length	1.0 inch.	25.40 mm.
r	Radius of the unbalance	1.2 inch.	30.50 mm.
W_J	Weight of the Journal	1.79 lb.	7.96 N
W_D	Weight of the disk	1.79 lb.	7.96 N
γ	Specific gravity of the oil	0.81	
μ_N	Nominal oil's viscosity	0.002250 Pa.s at 20°C	

Table 2. Positions of the proximity probes relative to the right end of the shaft

Nomenclature	Description	Dimensions English unit	SI unit
Z_1	to P1	10.75 in.	27.30 cm.
Z_2	to P2	8.00 in.	20.32 cm.
Z_3	to P3	3.75 in.	9.52 cm.
Z_4	to P4	0.50 in.	1.27 cm.
Z_D	to the disk	9.38 in.	23.81 cm.
Z_{SFD}	to the SFD	6.00 in.	15.24 cm

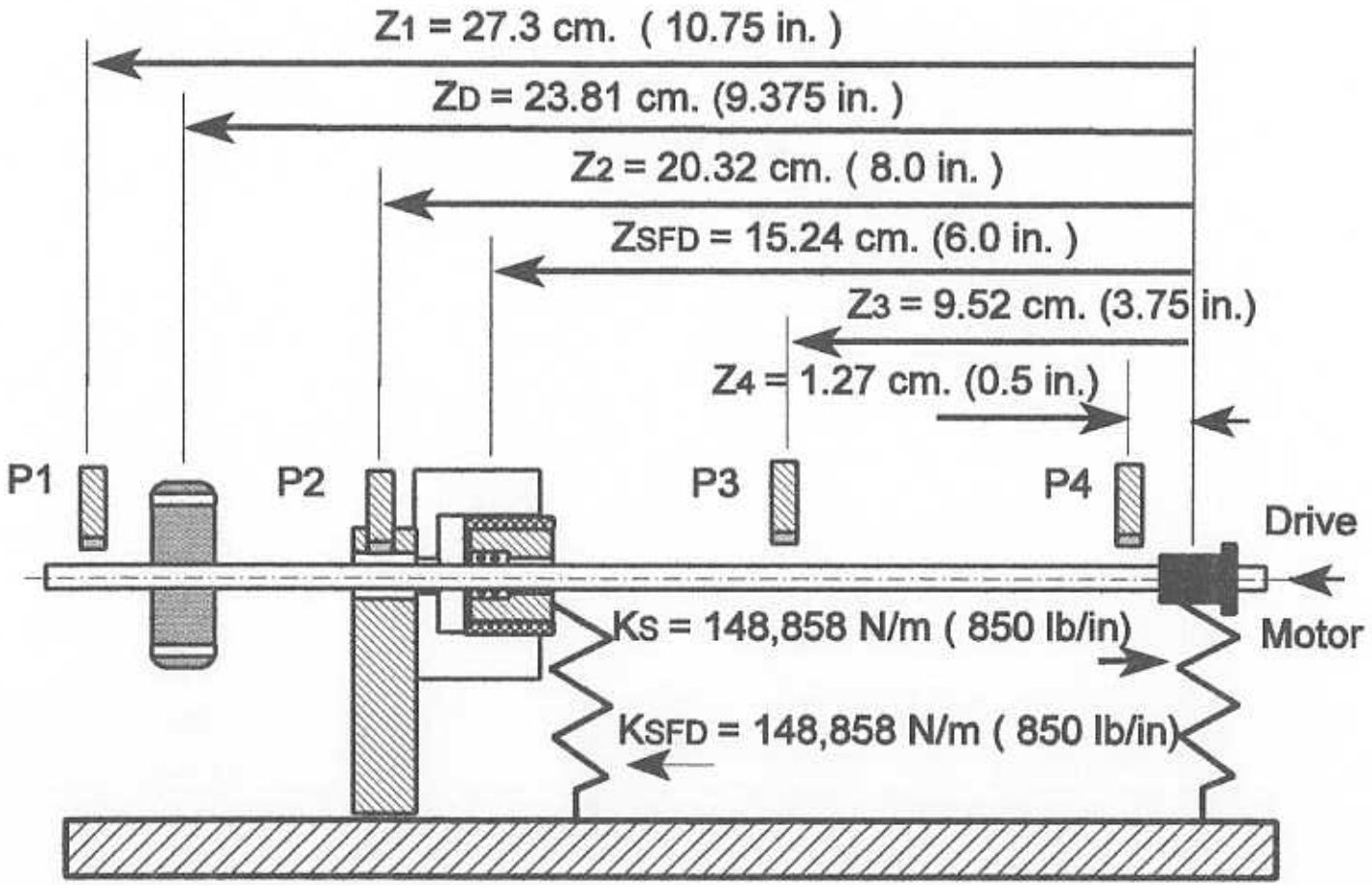

Figure 6. Rotor-SFD Test Rig : Location of displacement sensors

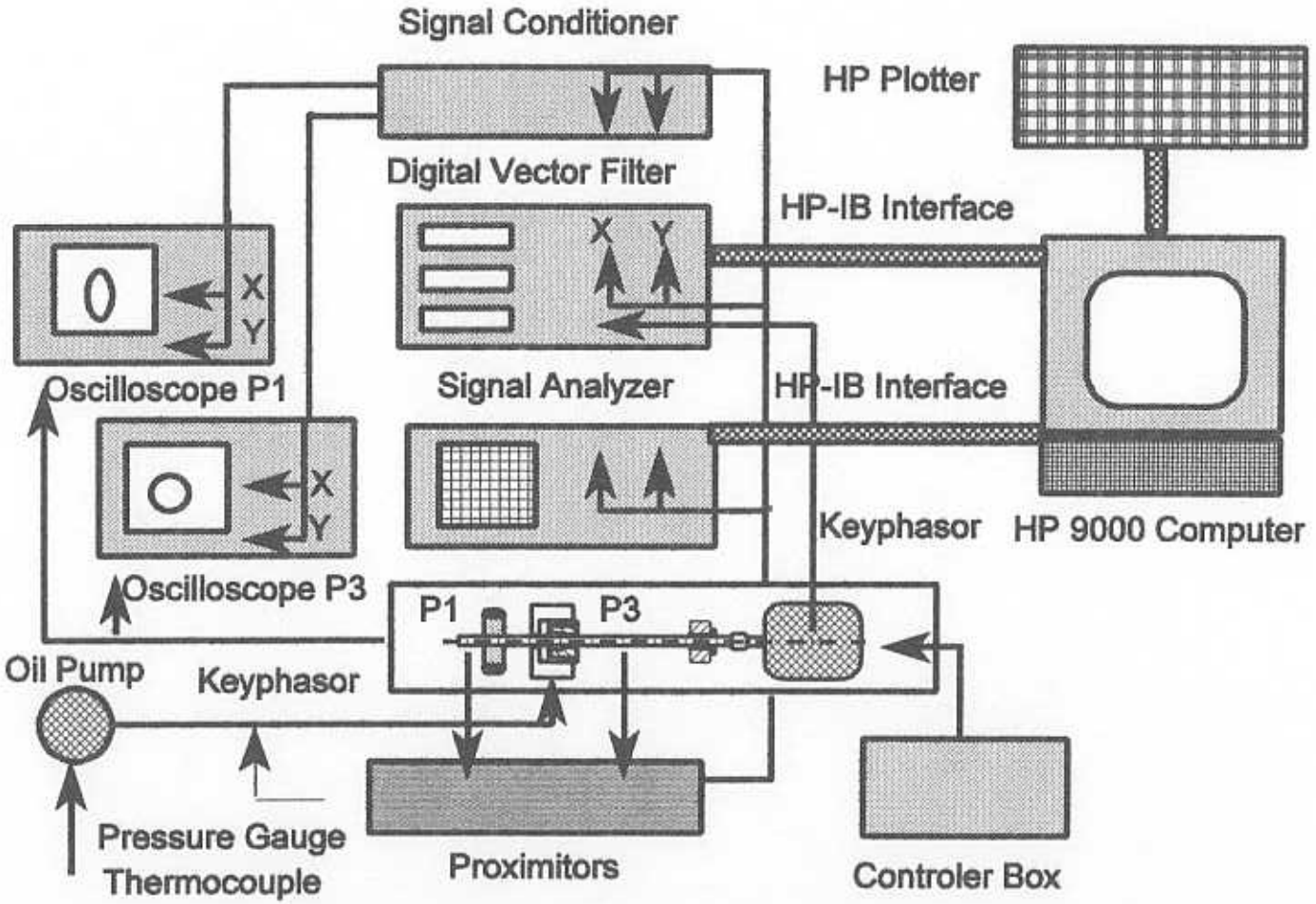

Figure 7. Schematic View of Instrumentation for Rotor-SFD Test Rig

gain of the transducers.

Table 3. Gain of the instrumentation transducers

Description	Gain	
	English unit	SI unit
Proximity probe	200 mV / mil	8 mV / μm
Pressure transducer	5 mV / psi	725 mV / MPa

Measurements of the system forced response to unbalance

San Andres, Laos and Lopez (1994) presented measurements of the unbalance response for a centered SFD. Damping coefficients were extracted from experimental data using a rigid rotor model operating in the conical mode. This report extends the measurements for the offcentered journal cases. Experimental measurements of the system dynamic forced response were performed for increasing levels of disk unbalance as the rotor coasted down from a top speed of 5,000 rpm and at a constant deceleration rate equal to 3,800 rpm/min. The lubricant to the damper was kept at a level of pressurization equal to 3.5 10^4 Pa (5 psi) above ambient and at an inlet temperature of approximately 29.5° C (85° F) with a nominal fluid viscosity of 0.00225 Pa.s.

Figure 8 shows the vertical and horizontal rotor responses measured at location P1 and P3 for unbalance masses corresponding to 1.0, 2.0 and 2.7 grams inserted on the disk at a radial distance equal to 30.5 mm (1.2 inches). Note that the experimental results shown in this Figure correspond to a SFD centered within the bearing housing i.e. the static journal center displacement is null. The curve labeled 0 grams corresponds to the base line trim balanced rotor response. Figures 9 and 10 show the unbalance response for conditions in which the journal center was statically displaced (offcentered) to 30% and 60% of the radial clearance. The displacement was vertical (upward) and produced by the soft spring attached to the squirrel cage base plate. The response curves presented show peak-to-peak amplitudes without any synchronous filtering.

Figure 11 shows frequency cascade plots of the vertical response at location P1 as the system speed decreases for a disk unbalance mass equal to 2.7 grams. The results of the centered journal and the 30% offcentered case, shown on Figures 11(a) and 11(b), show no trace of asynchronous frequency components in the unbalance response at location P1. The frequency response curve shown in Figure 11(c) for the 60% offcentered journal shows a supersynchronous frequency response that tracks at twice the rotational speed,. This effect can not be attributed to rotor misalignment because for the other cases it never showed up, so it follows that is only due to the offcentering of the damper journal.

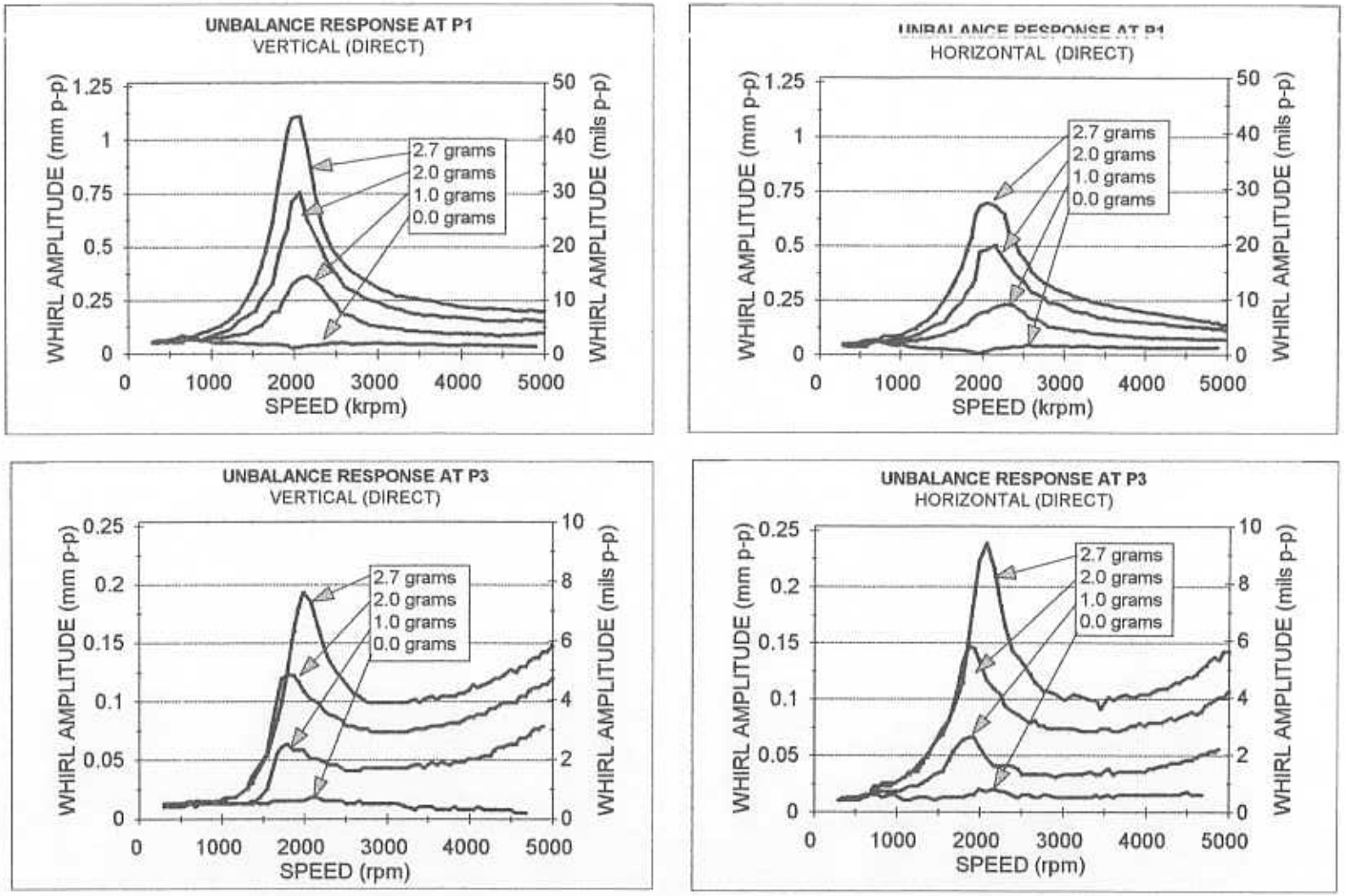

Figure 8. Rotor unbalance response at locations P1 and P3 (vertical and horizontal directions) for disk unbalance masses of 0.0, 1.0, 2.0 and 2.7 grams. Journal centered

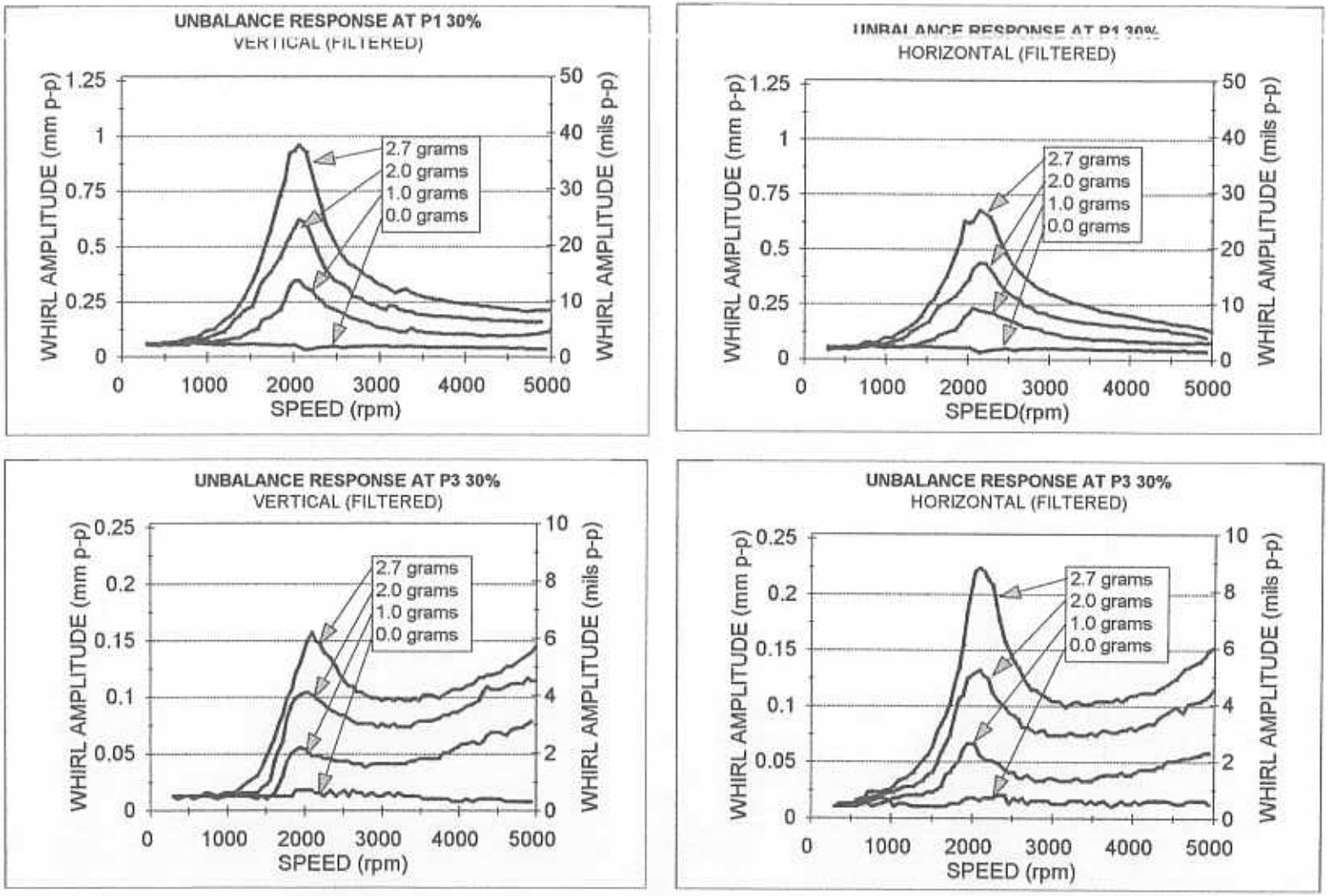

Figure 9. Rotor unbalance response at locations P1 and P3 (vertical and horizontal directions) for disk unbalance masses of 0.0, 1.0, 2.0 and 2.7 grams
Journal static displacement: 30% of radial clearance

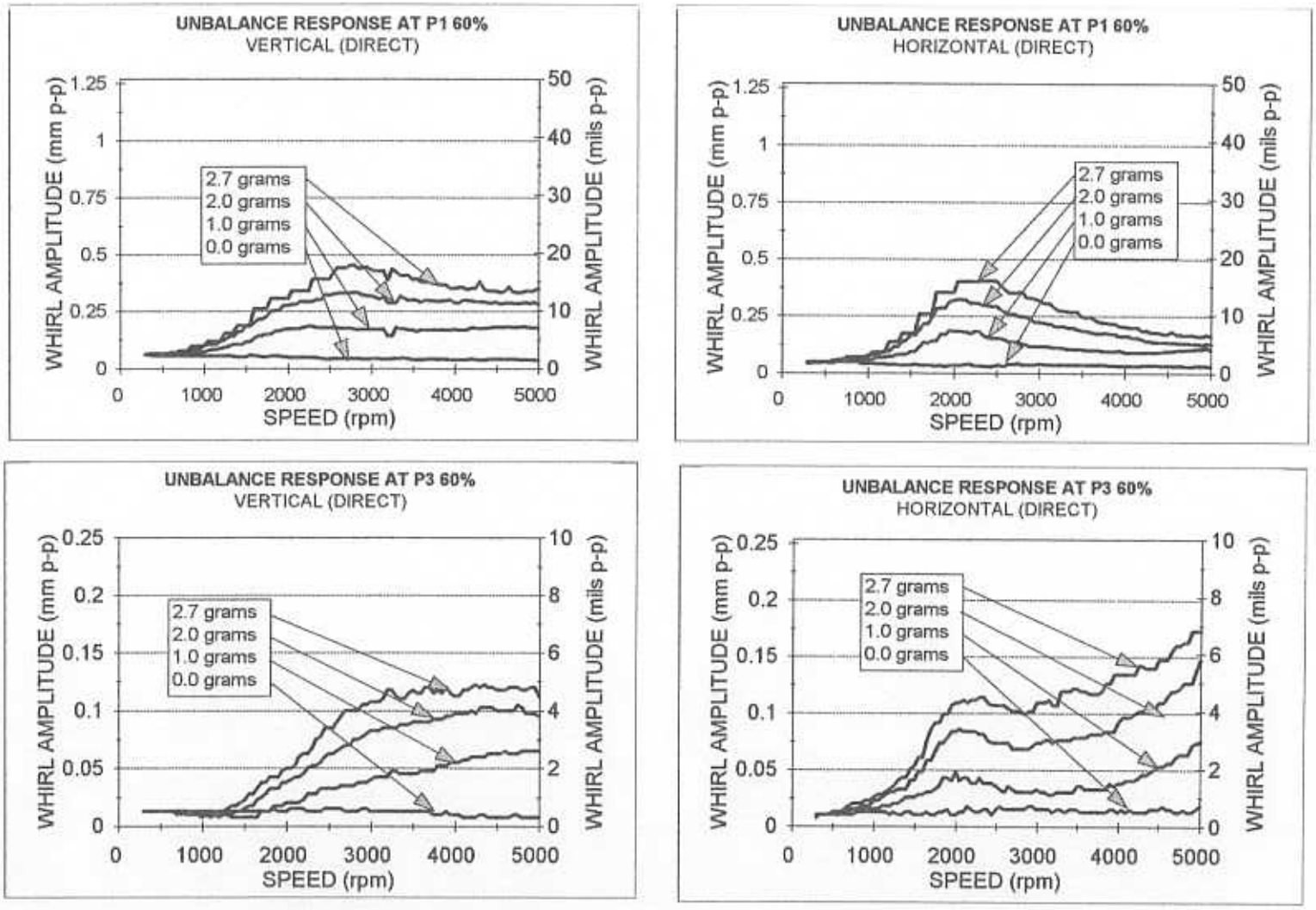

Figure 10. Rotor unbalance response at locations P1 andP3 (vertical and horizontal directions) for disk unbalance masses of 0.0, 1.0, 2.0 and 2.7 grams
Journal static displacement: 60% of radial clearance

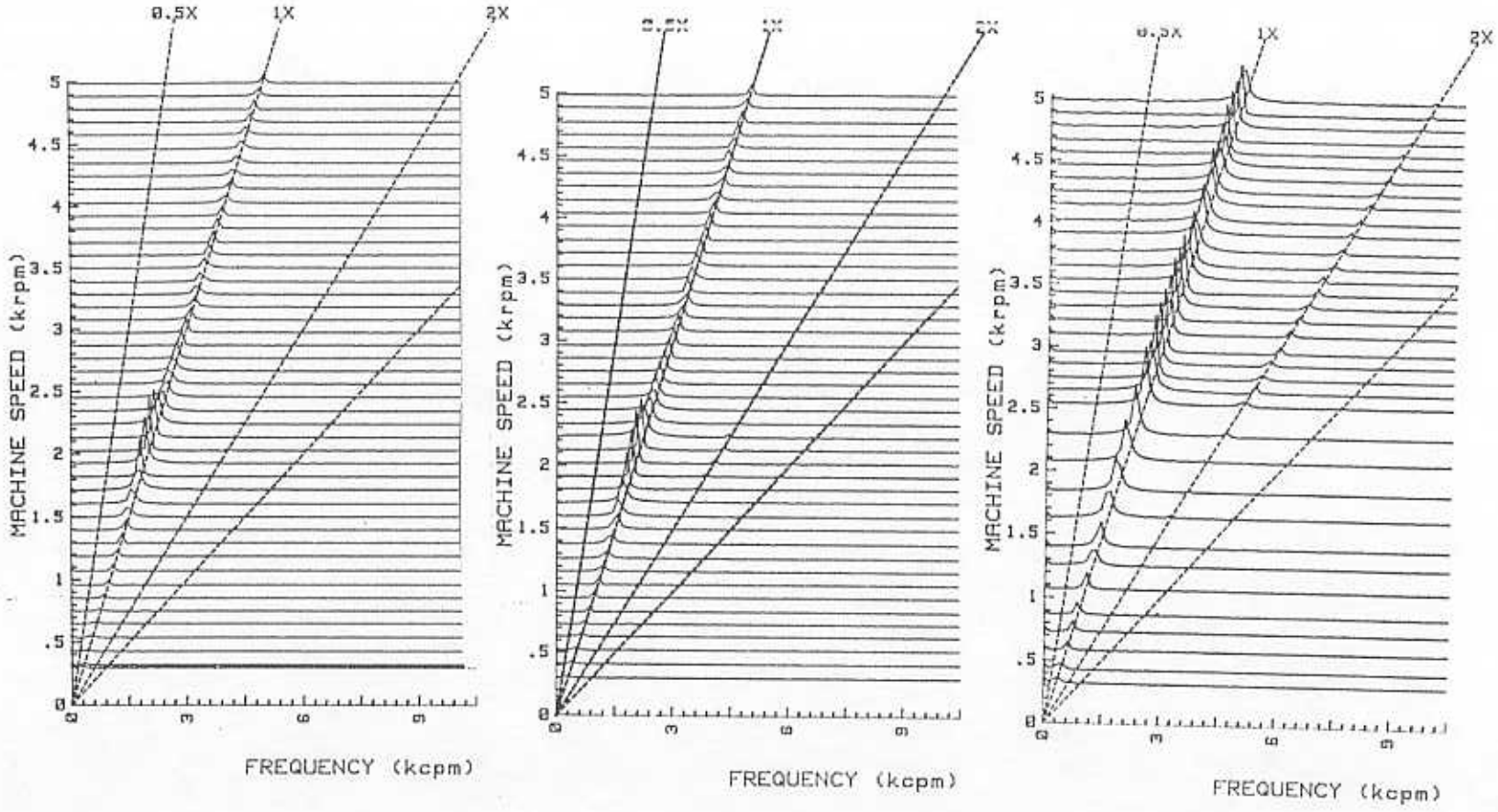

Figure 11. Frequency response plots of the vertical response at P1 with an unbalance mass of 2.7 grams
(a) Journal centered
(b) Journal static displacement: 30% of radial clearance
(c) Journal static displacement: 30% of radial clearance

The measurements from the unbalance response, in the centered journal case, show that at the critical speed the vertical amplitude of motion is about 1.25 times the horizontal response, and consequently, the shaft orbits at location P1 are elliptical as a probable consequence of the damping asymmetry on the SFD. The asymmetry of the squirrel cage support stiffness is too low to be considered a significant factor. Also, Figure 8 shows the vertical and horizontal response at location P3 for the same conditions of disk unbalance as detailed above. The ratio of horizontal to vertical peak-to-peak amplitudes is also approximately equal to 1.25. At location P3 for the largest rotor speeds, the vibration amplitudes start to increase since the rotor-damper system is approaching its second critical speed (approximately at 6,960 rpm) and which corresponds to the first flexural mode. Similar ratios of maximum amplitudes are observed for the offcentered journal case of 30%. It is worth to mention that the static offcentering was achieved with an accurancy of ±12.7 μm (0.5 mils).

Figure 10 corresponding to the 60% offcentered journal case shows in the vertical and horizontal directions an amplitude of motion that appears to be highly damped when compared with the previous cases. The ratio of amplitudes at P1 (vertical vs. horizontal) is 1.15 denoting an orbit that is almost circular. At P3 the ratio of amplitudes (horizontal vs. vertical) is 2.0 at the critical speed but this value decreases to close to 1.0 as the speed is increased. Note also that the location of maximum amplitude vibration and which defines the system first critical speed shifts (slightly) towards higher speeds as the disk unbalance level increases. This observation appears to confirm that the squeeze film damper provides a small radial stiffness as the SFD operating dynamic journal eccentricity increases.

Figure 12 shows the maximun peak-to-peak amplitudes of motion at P1 and P3 as a function of the unbalance masses for the centered and offcentered journal cases. From this curves it follows that the relation between the maximum amplitude and the unbalance masses is linear for most cases, except for the largest unbalance masses used. The experimental results demostrate that offcentering the SFD journal effectively increases the damping in the system.

Unbalance response using a rotordynamics program

A commercial rotordynamics computer code (PUP) was used to predict the unbalance response at locations P1 and P3 of the rotor-SFD test apparatus. This computational program is based on the transfer matrix method for the calculation of the unbalance response (Murphy and Vance,1983). For the analysis, the rotor shaft was divided into 9 stations with stiffness coefficients equal to 850 lb/in at the two bearing support locations. The values of the damping coefficients were then obtained by trial and error using the criteria to reproduce the similar unbalance response curves as those obtained from the experiments. Table 4 shows the estimated damping coefficients at the

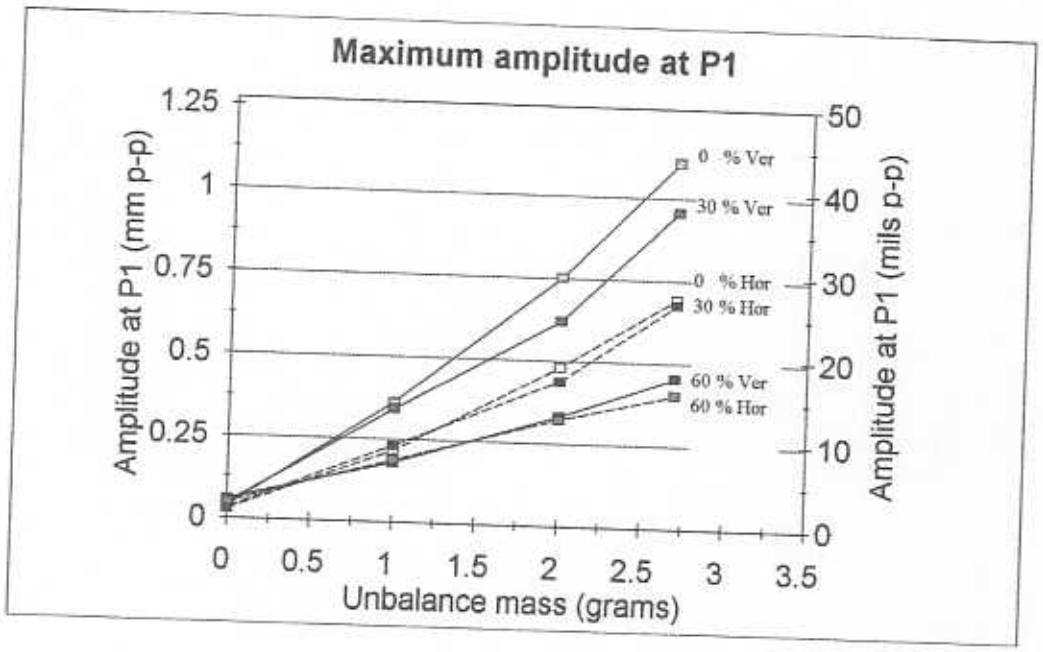

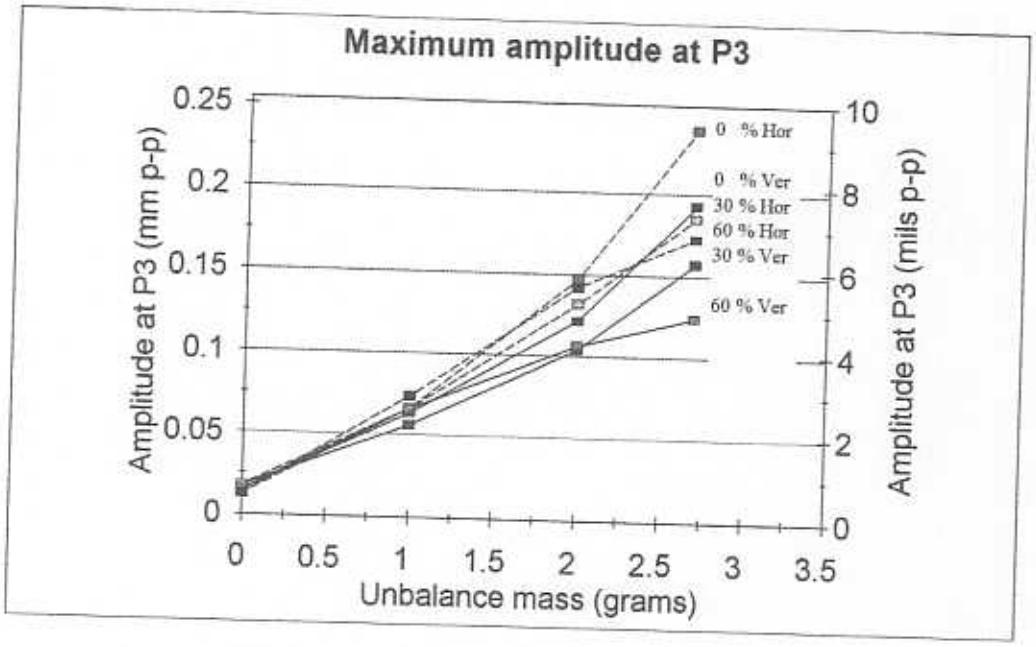

Figure 12. Maximum amplitudes of motion at P1 and P3 as a function of the unbalance masses

journal cases.

Table 4. Estimated damping coefficients used in the unbalance response program (PUP)

CASE	horizontal direction C_{xx} (N.s/m)	(lb.s / in)	vertical direction C_{yy} (N.s/m)	(lb.s / in)
Centered journal	350.25	2.00	210.15	1.20
Offcentered journal 1	385.28	2.20	227.67	1.30
Offcentered journal 2	612.95	3.50	788.10	4.50

where the two offcentered journal cases correspond to an upward static displacement of the journal of 30 and 60% within the bearing clearance. The values provided in Table 4 are insensitive to the unbalance mass.

Results from the predicted unbalance response at locations P1 and P3 for different unbalance masses and for the centered and offcentered journal cases are shown on Figures 13, 14 and 15. The following provides a comparison of the experimental data and the numerical model predictions:

Centered case at the critical speed: As shown in Figure 13 the predicted amplitudes at location P1 in the vertical direction are similar to the experimental results depicted on Figure 8. The calculated amplitudes at location P3 in the vertical direction (Figure 13) are about 75% of the measured amplitudes (Figure 8). The differences are larger on the horizontal direction where the predicted amplitudes at location P3 (Figure 13) are about 40% of the measured amplitudes (Figure 8).

Centered case at maximum speed: In the vertical direction the predicted amplitudes at location P1 (Figure 13) are similar to the experimental results (Figure 8). However, in the horizontal direction, the predicted amplitudes at location P1 (Figure 13) are 100% higher than the measured amplitudes (Figure 8). The predicted amplitudes in the vertical direction at location P3 (Figure 13) are similar to the measured amplitudes (Figure 8). In the horizontal direction at location P3 the predicted amplitudes (Figure 13) are very similar to the measured amplitudes (Figure 8).

Offcentered journal at 30% of radial clearance at the critical speed: The predicted amplitudes at location P1 in the vertical and horizontal directions (Figure 14) are similar to the measured amplitudes (Figure 9) *. The predicted amplitudes at location P3 in the

* Same observation detailed for centered case

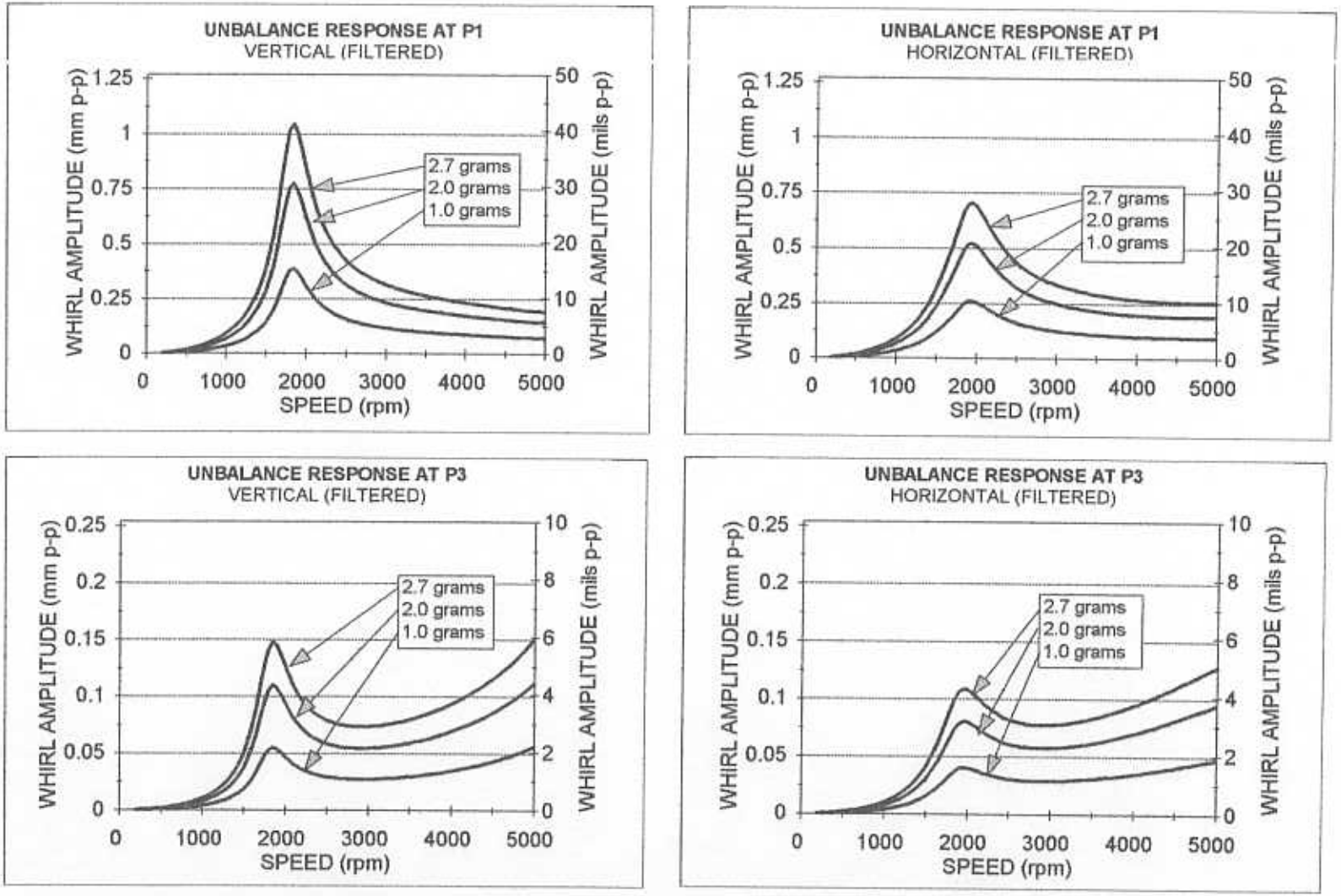

Figure 13. Results from the model for the unbalance response at locations P1 and P3 (vertical and horizontal directions) for disk unbalance masses of 0.0, 1.0, 2.0 and 2.7 grams Journal centered

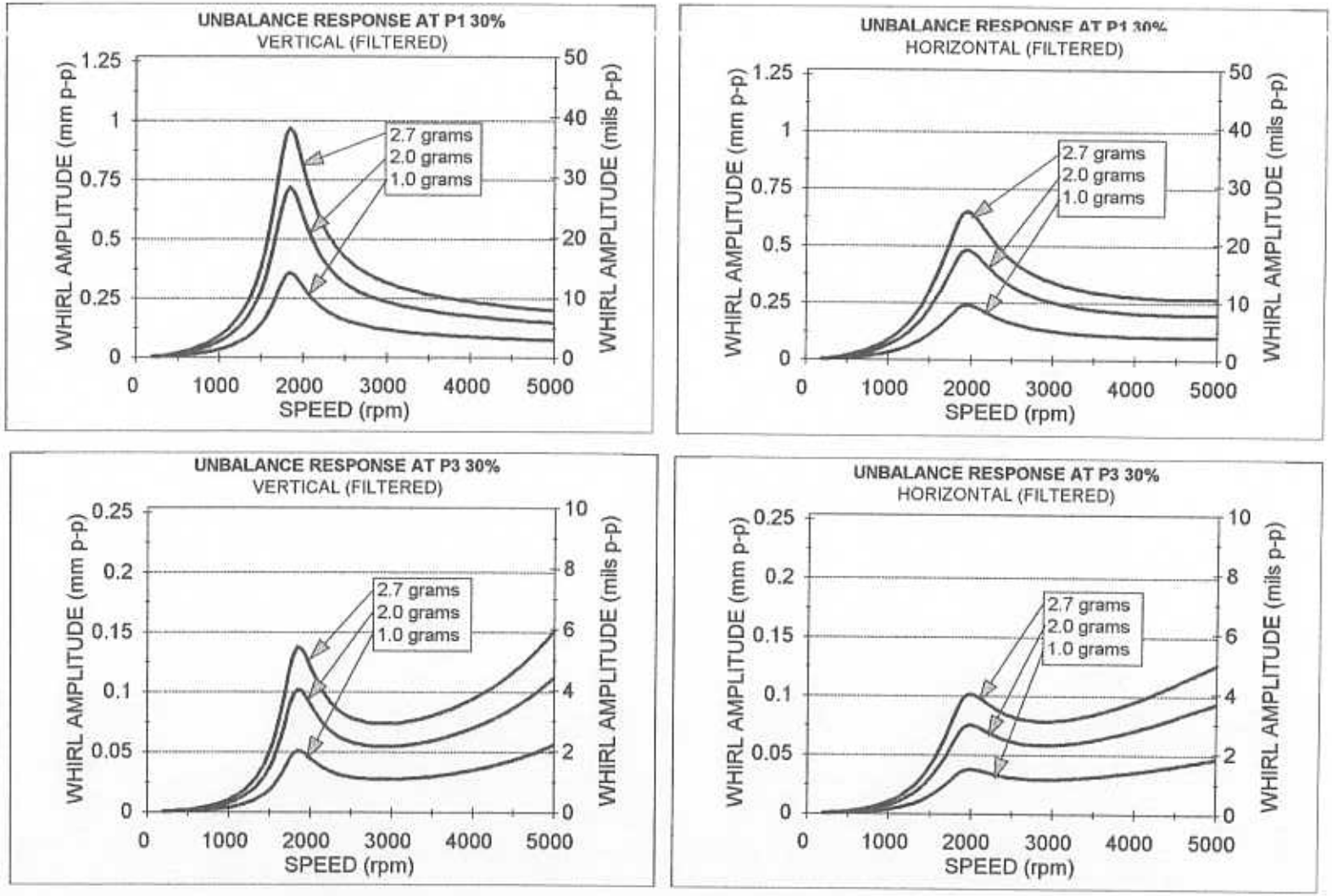

Figure 14. Results from the model for the unbalance response at locations P1 and P3 (vertical and horizontal directions) for disk unbalance masses of 0.0, 1.0, 2.0 and 2.7 grams
Journal static displacement: 30% of radial clearance

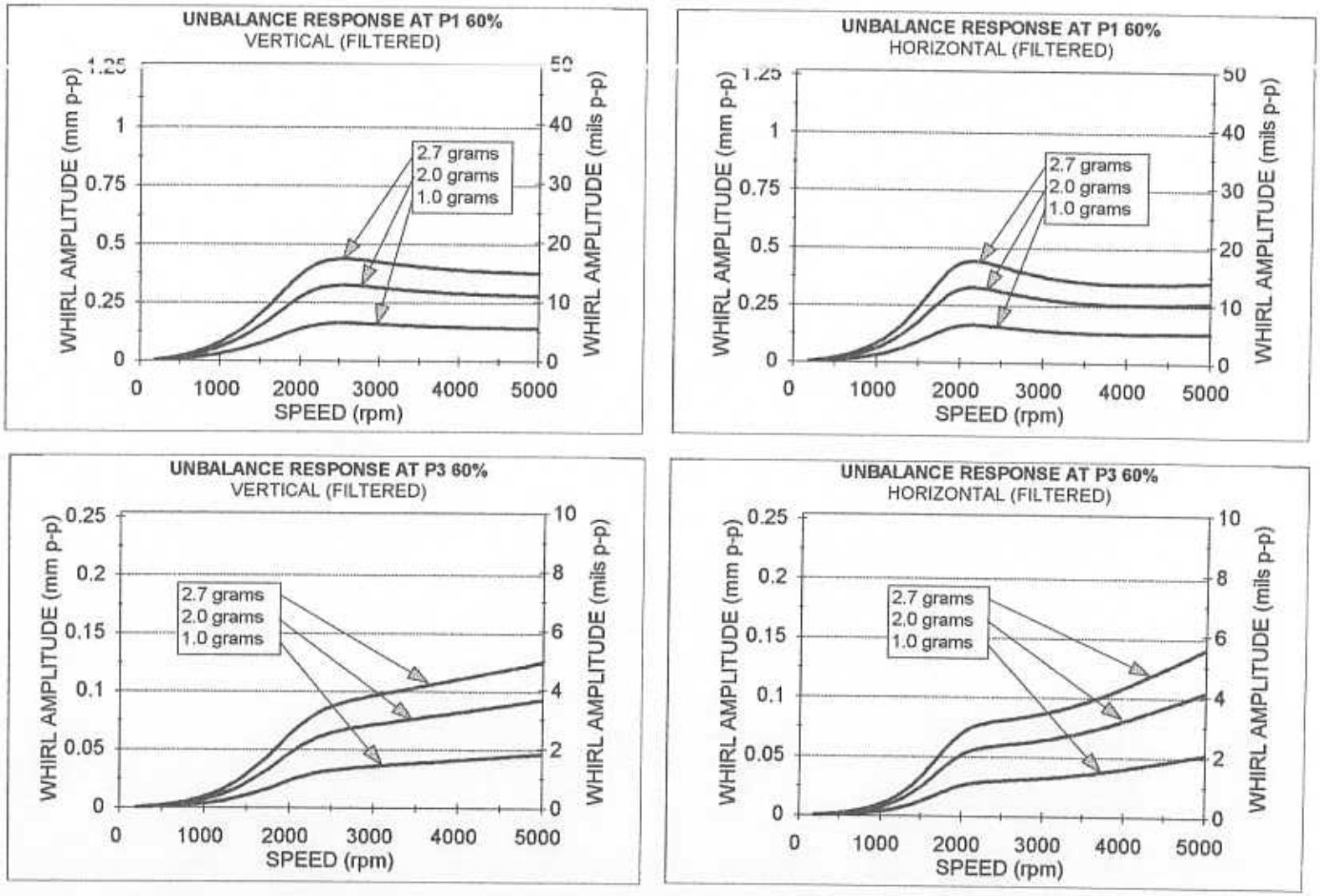

Figure 15. Results from the model for the unbalance response at locations P1 and P3 (vertical and horizontal directions) for disk unbalance masses of 0.0, 1.0, 2.0 and 2.7 grams Journal static displacement: 60% of radial clearance

vertical direction (Figure 14) are similar to the measured amplitudes at P3 (Figure 9). In the horizontal direction the predicted amplitudes at location P3 (Figure 14) are 40% of the measured amplitudes (Figure 9) *.

Offcentered journal at 30% of radial clearance at the maximum speed: In the vertical direction the predicted amplitudes at location P1 (Figure 14) are similar to the measured amplitudes (Figure 9) *. But, in the horizontal direction at location P1 the predicted amplitudes (Figure 14) are 100% higher than the measured amplitudes (Figure 9) *. The predicted amplitudes in the vertical and horizontal direction at location P3 (Figure 14) are similar to the measured amplitudes (Figure 9) *.

Offcentered journal at 60% of radial clearance at the critical speed: The predicted amplitudes at location P1 in the vertical and horizontal directions (Figure 15) are similar to the measured amplitudes (Figure 10) *. The predicted response at location P3 in the vertical direction at the critical speed cannot be compared with the measured amplitude (Figure 10) since the system is overdamped. In the horizontal direction the predicted amplitudes at location P3 (Figure 15) are about 60% of the measured amplitudes (Figure 10).

Offcentered journal at 60% of radial clearance at the maximum speed: In the vertical direction the predicted amplitudes at location P1 (Figure 15) are similar to the measured amplitudes (Figure 10) *. But, in the horizontal direction at location P1 the predicted amplitudes (Figure 15) are 100% higher than the measured amplitudes (Figure 10) *. The predicted amplitudes in the vertical direction at location P3 (Figure 15) are similar to the measured amplitudes (Figure 10) *. In the horizontal direction the predicted amplitudes at location P3 (Figure 15) are 80% of the measured amplitudes (Figure 10).

The comparisons performed (experiment vs. theory) show many similarities between the different cases tetsed. These are especially good at location P1 except at the largest speed in the horizontal direction. The best comparisons at location P3 were for the largest speed in both directions (X&Y). The comparisons also demonstrate the effective use of a rotordynamic program to simulate the behavior of the test apparatus.

More accurate results from the rotordynamics model could be obtained by assigning different values of damping coefficients at several rotational speeds. This procedure could certainly modify the amplitudes of motion observed at the largest operating speed. Also, the results could be improved with the use of angular-stiffness coefficients at the squirrel cage location.

---

* Same observation detailed for centered case

SFD force coefficients based on lubrication theory

The SFD damping coefficients are evaluated depending on the characteristics of the system. Most applications correspond to a journal centered and the most common model used corresponds to the short length, π film cavitated solution. This formulation is only valid on the assumption that half the pressure distribution has zero value due to the effect of the oil cavitation.

Figure 16 shows the measured pressure vs. time curve at the SFD location collected with a pressure transducer. This plot was obtained at an oil inlet pressure of 7.6 10^4 Pa (11 psi), rotational speed of 2050 rpm corresponding to the critical speed and with an unbalance mass of 2.7 grams. It is observed that the oil film pressure does not show vapor cavitation. Hovewer, the lubricant within the damper film lands, and as the system passed through the first critical speed (2050 rpm), was observed to have a non-uniform behavior, generating a "burping" sound as if oil bubbles were collapsing under the dynamic action of the journal motion. The lubricant did not fill the entire film lands and the phenomena appeared to be chaotic in nature.

Thus, for the current test results it is not possible to assume the π film cavitated model. The direct (C_{tt}) and cross coupled (C_{rt}) damping coefficients are defined by the following expressions based on the uncavitated (2π film) solution for the short length, open ends SFD model (Vance,1988):

$$C_{tt} = \frac{\mu R \left(\frac{L}{C}\right)^3 \pi}{(1-\varepsilon^2)^{\frac{3}{2}}} \qquad C_{rt} = 0 \qquad (1)$$

where $\varepsilon = e / C$ is the dimensionless orbit radius or journal dynamic eccentricity. Note that the cross-coupled coefficient is null. All the variables necessary to solve equation (1) have been previously defined with the exception of the dimensionless orbit radius. There is no experimental data of the vibrational amplitude at the SFD location, so the amplitudes are evaluated with the help of the rotordynamic model.

Figure 17 shows the calculated rotor deflected shapes in the horizontal and vertical directions obtained from the rotordynamic model. The second column of Table 5 shows the average value of the horizontal and vertical amplitudes at the SFD location. The last column corresponds to the theoretical damping coefficients obtained using equation (1). Note the large variation on theoretical damping coefficients as orbit radius increases. The average value of the direct damping coefficient (C_{tt}) is 171.37 N.s/m (0.978 lb.s/in) and recall the estimated damping coefficient from the mathematical modeling of the test data

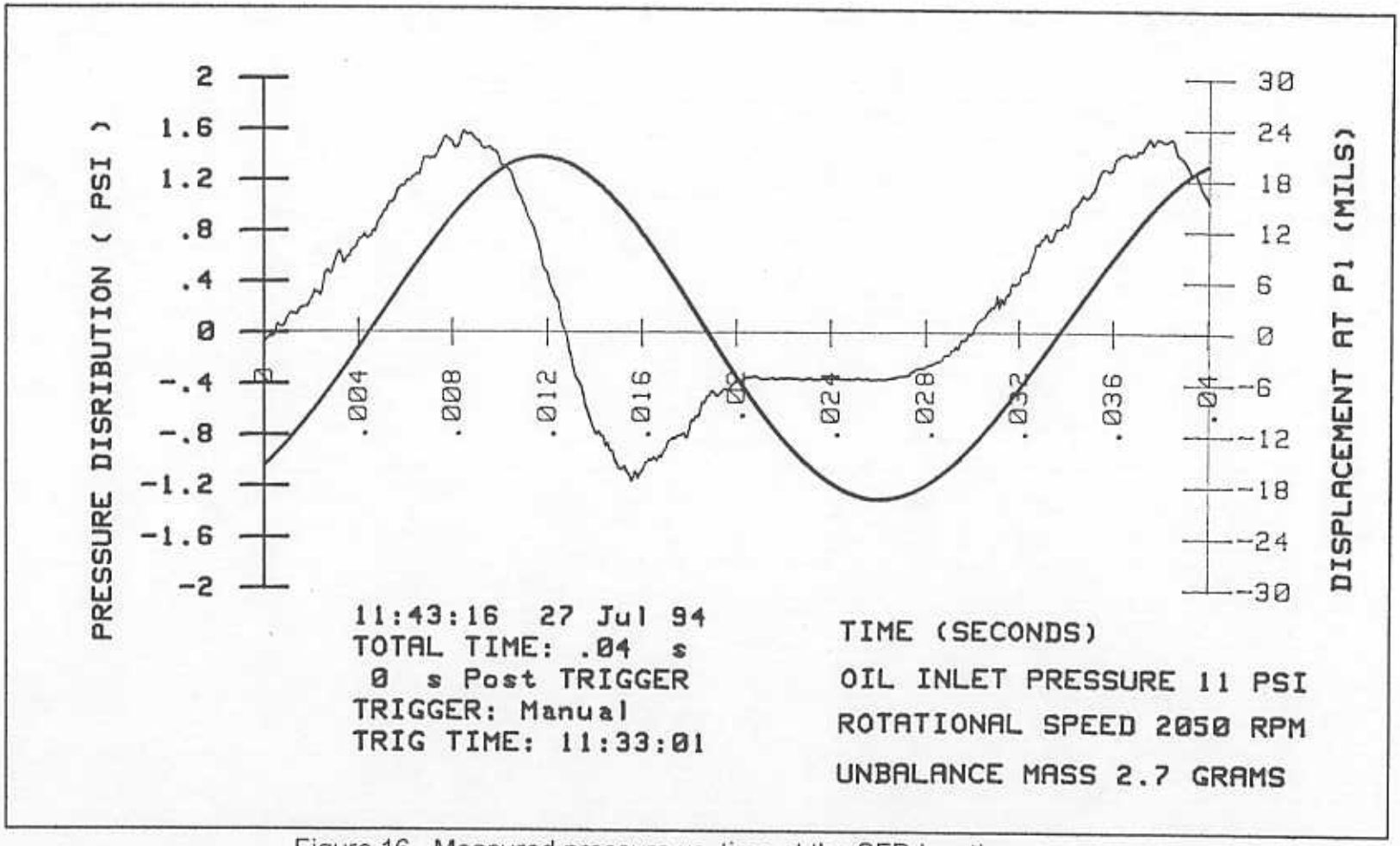

Figure 16. Measured pressure vs. time at the SFD location.
oil inlet pressure 7.6 10^4 Pa (11 psi).
the maximum amplitude at P1 corresponds to the
minimum fluid film clearance at the SFD location.

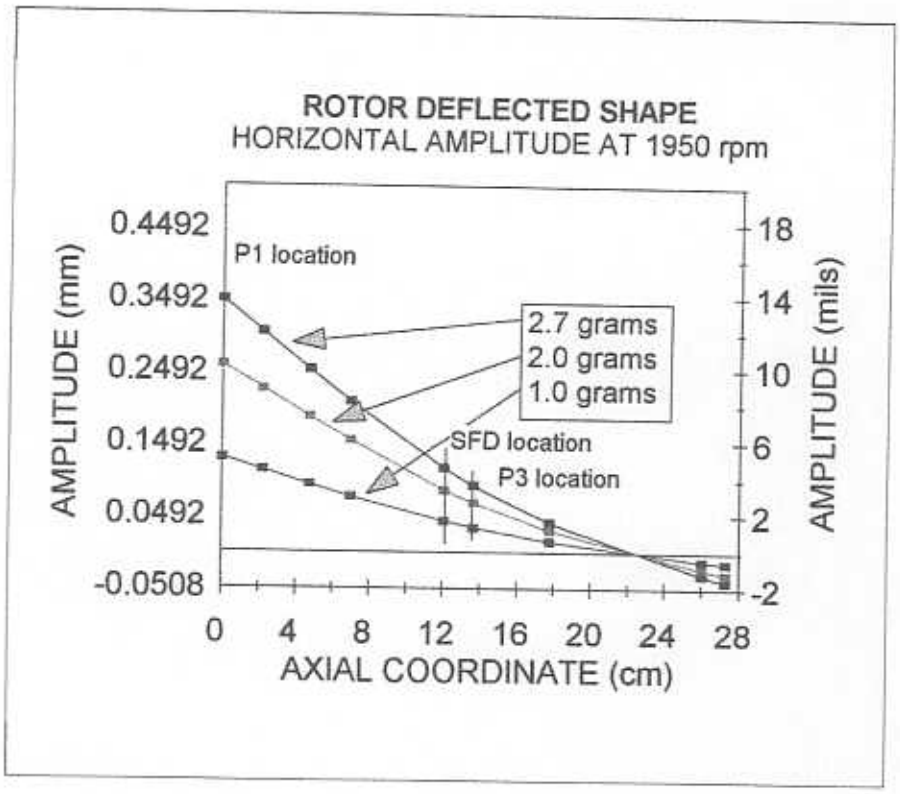

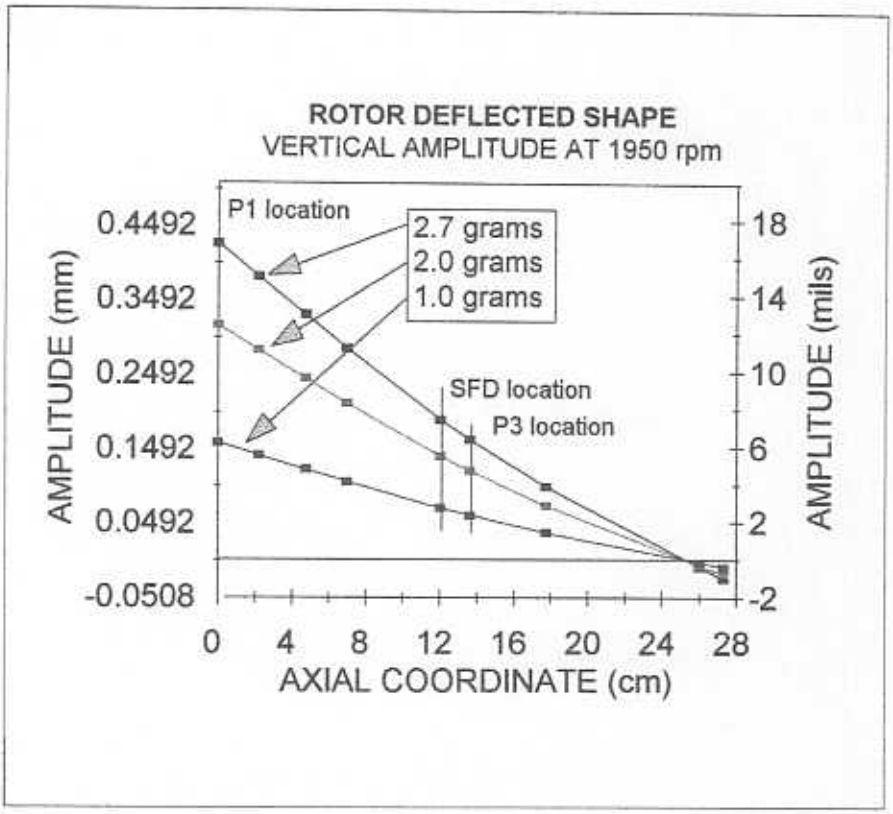

Figure 17. Rotor deflected shapes in the horizontal and vertical directions obtained from the rotordynamic model Centered journal case

for the centered case is equal to 210.15 N.s/m (1.20 lb.s/in) as given in the first entry of Table 4.

Table 5. Damping coefficients calculated using the 2π film model at the SFD location for the critical speed (1950rpm). Centered journal case, [C = 0.28 mm (11 mils)]

m_u (grams)	Amplitude at the SFD (mm)	(mils)	ε (e/C)	C_{tt} (N.s/m)	(lb.s/in)
2.7	0.1530	6.02	0.547	230.08	1.314
2.0	0.1133	4.46	0.405	176.60	1.008
1.0	0.0566	2.23	0.203	143.90	0.820
0.0	0.00	0.00	0.000	171.37	0.770

A SFD program was also used to calculate the damping coefficients for the statically offcentered cases (San Andres and Vance, 1987). Figure 18 shows the results of the damping and mass coefficients vs. static journal eccentricity ratio for the non-cavitated formulation. Table 6 presents the theoretical results for each one of these cases. It is worth to mention that the predicted values for the offcentered case are strictly valid for small amplitude journal motions about an offcentered equilibrium position.

Table 6. Damping coefficients calculated from the SFD code (San Andres and Vance, 1987)

CASE	horizontal direction C_{xx} (N.s/m)	(lb.s / in)	vertical direction C_{yy} (N.s/m)	(lb.s / in)
Centered journal ε_s=0.0	122.70	0.70	122.70	0.70
Offcentered journal ε_s=0.3	137.70	0.78	178.40	1.02
Offcentered journal ε_s=0.6	210.40	1.20	558.40	3.19

Table 7 shows the ratio of the damping coefficient values obtained from the rotordynamic code (Table 4) over the analytical values (Table 6). At Table 7 is observed that the damping coefficient ratio, on each direction, appear to be consistent.

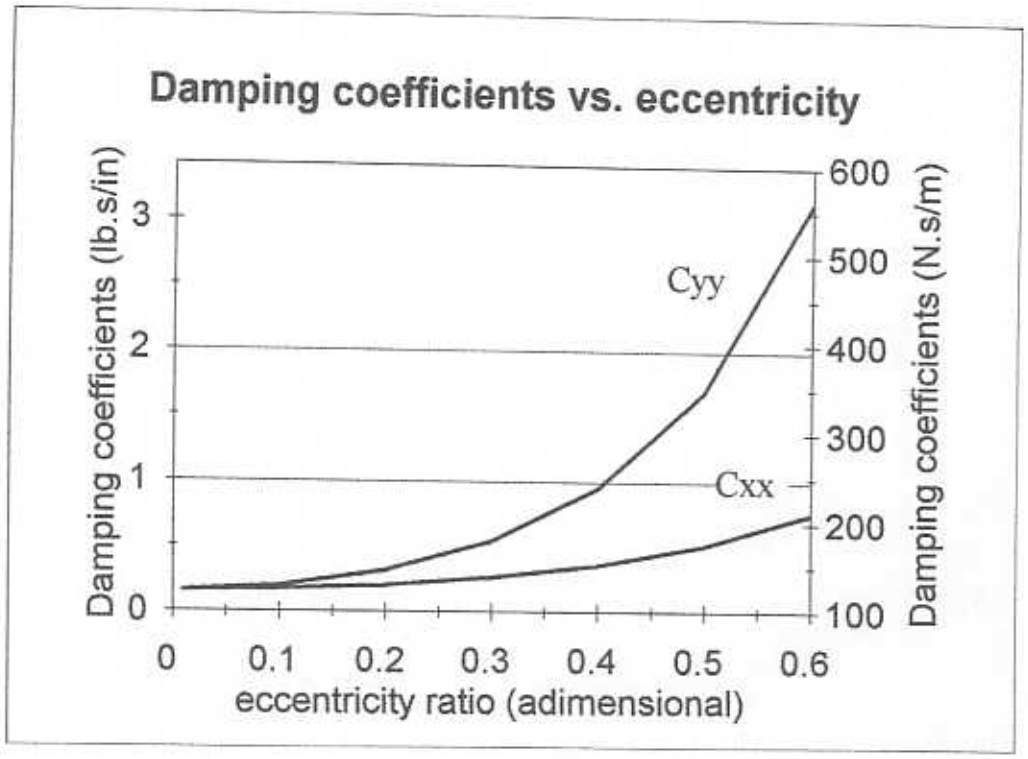

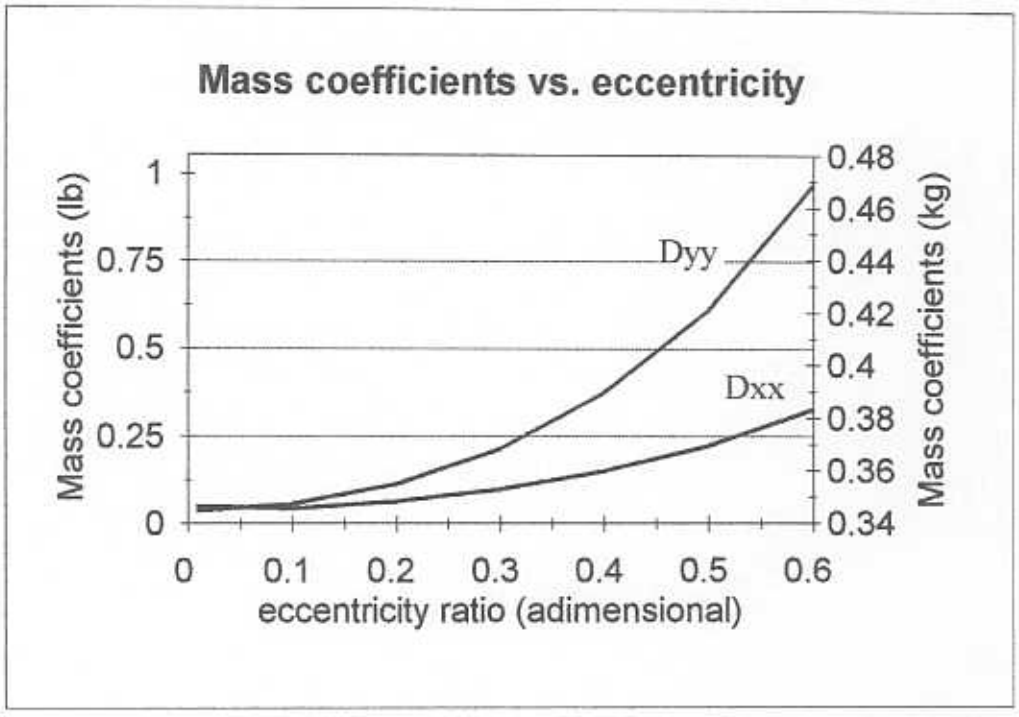

Figure 18. Damping and mass coefficients vs. static journal eccentricity ratio. calculated from SFD code (non-cavitated).
(San Andres and Vance, 1987)

Table 7. Damping coefficients ratio
(estimated vs. theoretical damping coefficients)

CASE	horizontal direction	vertical direction
Centered journal ε_s=0.0	2.86	1.71
Offcentered journal ε_s=0.3	2.82	1.27
Offcentered journal ε_s=0.6	2.91	1.41

Conclusions

The test rig consists of a shaft supported by an O'ring bronze bushing (at the motor side) and by a SFD support. The disk located at the end of the shaft provided the location for unbalance weights. The overhung rotor configuration used for the SFD-rotor-kit apparatus proved to be a very good and reliable source of experimental data. It is important to note that the high quality of the measured unbalance responses was a consequence of the time inverted in the leveling of the rotor, alignment of the supports, balancing of the rotor disk, and centering of the damper.

The results from the experiments show that the maximum amplitudes of unbalance response are directly related to the amount of the unbalance mass. Statically offcentering the journal increases the damping in the system and reduces considerably the rotor amplitudes of motion.

Good agreement was found between the experimental unbalance responses and the results from a linear rotordynamic model. This agreement was especially good at the rotor location closest to the end disk, in the vertical and horizontal directions, with the only exception at high speeds in the horizontal direction. The measurements at the shaft midspan didn't show a good correlation probably because the rotordynamic model has to be refined to include damping coefficients at several speeds.

The conventional short length SFD, full film model determines damping coefficients as a function of the orbit radius. However, the estimated damping coefficients from the test apparatus appear to be insensitive to the rotor amplitude of motion.

The ratio of the non-cavitated damping coefficients estimated from the rotordynamic model vs. the damping coefficients obtained from a prior analysis are consistent and larger than one. Then a good estimation of the damping values at the horizontal and vertical directions for the rotordynamic code could be obtained by multiplying the damping coefficients obtained from the theoretical analysis by the scale factors of 2.86 and 1.46 in

the horizontal and vertical directions respectively.

REFERENCES

[1] Childs,D.W.,(1993),"Turbomachinery Rotordynamics: Phenomena, Modeling, and Analysis," Wiley Interscience Pubs., pp.216.

[2] Ehrich,F.F.,(1992),"Handbook of Rotordynamics," Mc Graw-Hill Pubs., pp. 2.41.

[3] Murphy,B. T., Vance,J.M.,(1983),"An Improved Method for Calculating Critical Speeds and Rotordynamic Stability of Turbomachinery," Journal of Engineering for Power, Vol. 105, pp. 591-595.

[4] San Andres,L.A., Laos, H.E., Lopez,A.,(1994),"Measurement of Unbalance Response in a SFD-Rotor Kit- Centered Damper," Research Progress Report to the Turbomachinery Research Consortium, TAMU, College Station, TRC-SFD-4-94, #125.

[5] San Andres,L.A., and Vance,J.M., (1987),"Effect of Fluid Inertia on Squeeze Film Damper Forces for Small Amplitude Circular Centered Motions," ASLE Transactions, Vol. 30, N° 1, pp. 69-76.

[6] Vance,J.M.,(1988),"Rotordynamics of Turbomachinery," Wiley Inter-Science Pubs., pp. 237.